Research article

Comparison of dosimetry with magnetic resonance and computed tomography imaging delineation of surgical bed volume in breast cancer irradiation

M. Betti [a,b], L.C. Orlandini [a,c,*], C. Biagini [a,d], M. De Liguoro [a,e], L. Cionini [f]

[a] Medical Physics Department, Centro Oncologico Fiorentino, 50019, Sesto Fiorentino (FI), Italy
[b] Medical Physics Department, Pistoia, Azienda USL Toscana Centro, 51100, Pistoia (PT), Italy
[c] Radiation Oncology Department, Sichuan Cancer Hospital & Research Institute, Chengdu, Sichuan 610041, China
[d] Diagnostic Department, Diagnostic Institute Santo Stefano, 59100, Prato (PO), Italy
[e] Radiation Oncology Department, Azienda sanitaria Locale Asti, 14100, Asti (AT), Italy
[f] Radiation Oncology Department, Centro Oncologico Fiorentino, 50019, Sesto Fiorentino (FI), Italy

HIGHLIGHTS

- Feasibility of using MRI for boost identification in breast irradiation in a clinical workflow.
- Improving boost dosimetry and avoiding hot or cold regions in the target breast volume.
- Evaluation of MRI and CT boost volumes in breast irradiation with a quantitative metric.

GRAPHICAL ABSTRACT
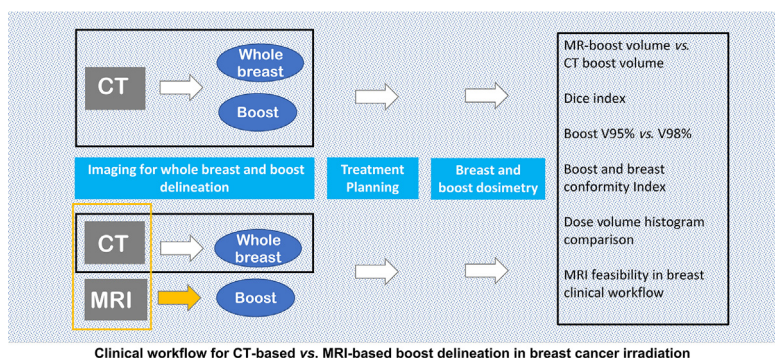
Clinical workflow for CT-based vs. MRI-based boost delineation in breast cancer irradiation

ARTICLE INFO

ABSTRACT

Background: Postoperative radiotherapy after conservative surgery for patients with breast cancer usually includes focal over-irradiation (boost) to the surgical bed (SB). Irradiation planning using computed tomography (CT) is difficult in many cases because of insufficient intrinsic soft tissue contrast. To ensure appropriate radiation to the tumor, large boost volumes are delineated, resulting in a higher dose to the normal tissue. Magnetic resonance imaging (MRI) provides superior soft tissue contrast than CT and can better differentiate between normal tissue and the SB. However, for SB delineation CT images alone remain the pathway followed in patients undergoing breast irradiation. This study aimed to evaluate the potential advantages in boost dosimetry by using MRI and CT as pre-treatment imaging.
Methods: Eighteen boost volumes were drawn on CT and MRI and elastically co-registered using commercial image registration software. The radiotherapy treatment plan was optimized using the CT volumes as the baseline. The dose distributions of the target volumes on CT and MRI were compared using dose-volume histogram cutoff points.

---

* Corresponding author. Radiation Oncology Department, Sichuan Cancer Hospital & Research Institute, Chengdu, Sichuan 610041, China.
 E-mail address: lucia.orlandini@icloud.com (L.C. Orlandini).

Results: The radiation volumes to the SB varied considerably between CT and MRI (conformity index between 0.24 and 0.67). The differences between the MRI and CT boost doses in terms of the volume receiving 98% of the prescribed dose (V98%) varied between 10% and 30%. Smaller differences in the V98% were observed when the boost volumes were delineated using MRI.

Conclusion: Using MRI to delineate the volume of the SB may increase the accuracy of boost dosimetry.

Introduction

Breast conservative treatment is the standard of care for early-stage breast cancer and includes focal irradiation (boost) delivered to the surgical bed (SB) to reduce the risk of local recurrence. Accurately identifying and delineating the boost volume (BST) is critical in treatment planning for breast irradiation. The simultaneously integrated boost technique has been proposed for standard use in breast-conserving radiotherapy (RT) because of its dose-limiting capabilities, ease of implementation, reduced number of treatment fractions, and relatively low incidence of acute skin toxicity[1]. Boost localization is currently performed using computed tomography (CT). However, multiple studies have shown the limitations of single-modality imaging with interobserver differences in the definition of the lumpectomy cavity.[1–4] For instance, CT lacks intrinsic contrast between soft tissue structures; therefore, SB cavity identification may be less accurate in some patients. Further, multiple factors, including breast density, the interval between surgery and image acquisition, and the volume of the lumpectomy cavity, can limit the ability to distinguish the SB from normal breast when using CT.[1] This leads to significant inter- and intra-observer variations in boost delineation, particularly when the cavity is situated in the subareolar area or within dense glandular breast tissue.[3,5,6] The placement of surgical clips perioperatively at the margins of the surgical cavity, although strongly recommended to facilitate localization, does not eliminate the risk of incomplete irradiation, as they do not correspond exactly to the cavity edges.[7] Adding margins to the boost volume is a common solution to circumvent uncertainties in identifying the SB; however, this can increase the dose to the normal tissue and toxicity. Therefore, combining CT with another imaging modality, such as magnetic resonance imaging (MRI) for determining the radiation field may improve the accuracy. MRI provides superior soft tissue contrast compared to CT and can better differentiate between normal tissue and the postoperative SB.[8] Therefore, MRI is used for breast cancer screening and presurgical evaluation. However, it has not been widely used in treatment planning because of its high cost and lack of availability. Additionally, MRI can be strongly operator dependent and difficult to execute under RT conditions.[9,10] For example, associating MRI with CT requires performing breast MRI in a supine position, as performed at the simulation CT, which does not allow the use of dedicated phased-array breast coils and requires dedicated software for registration. Nevertheless, previous studies have found that supine breast MRI yields a more precise definition of the SB than CT with a smaller interobserver variability and may obviate the need for surgical clips; therefore, CT–MRI fusion should be used for SB delineation in patients undergoing partial breast irradiation.[11] Despite these evidences, the contextual use of a dual imaging modality at the treatment planning stage is not a common practice. In this study, we investigated the possibility within a clinical workflow of registering MRI on CT images to localize the SB for boost irradiation and quantitatively analyzed the impact on dosimetry for treatment planning.

Methods

Patient selection

We enrolled 18 patients undergoing breast-conserving surgery and breast irradiation in this retrospective study. The study was approved by the Ethics Committee of Centro Oncologico Fiorentino Hospital. Patients provided oral consent for the elaboration of the study data and future scientific publication.

Patient positioning and imaging

Patients were immobilized using CT/MRI-compatible customized Vac-Lok™ cushions (CIVCO Medical Solutions, Kalona, Iowa, USA) and KneeSTEP and FeetSTEP supports (IT-V, Innsbruck, Austria) for easy reproduction of the patient setup across MRI and CT studies, as well as for accurate positioning. All patients were scanned in the RT treatment position: supine with both arms in the abduction and the hands above the head. CT and MRI scans were performed on the same day. Three setup markers appropriate for each modality were placed, two lateral and one medial on the same skin points, to facilitate image fusion. Non-contrast CT axial images with 3-mm-slice thickness were acquired using a Somatom Definition AS (Siemens) scanner in the free-breathing mode. Magnetic resonance (MR) images were acquired in the same position, immediately after the CT scan, using a 3 T S Verio (Siemens Healthcare) scanner. For MRI, the free-breathing acquisition was impossible; therefore, an echo-navigator respiratory gating system was used, and the acquisition interval was fixed in the expiration phase to minimize deviations from CT scans. The field of view (FOV) in the longitudinal direction was typically from C4 to below the diaphragm. A 6-channel body matrix coil was anteriorly positioned and stabilized with Styrofoam blocks to avoid movement or displacement of the coil and compression or dislocation of the breast surface. Posteriorly, the FOV was spanned by a 24-channel Matrix Spine Coil. A gated three-dimensional variable-flip angle T2-weighted scan with repetition time of 1550 ms, effective echo time of 365 ms, a parallel imaging factor of 2, and a matrix of 256×192 (FOV 340×255 mm^2) was acquired to obtain axial images with 1.3-mm^3 isotropic voxels. The nominal sequence acquisition average time was 3 min and 44 s, and the total examination time was less than 20 min for every patient. MR and CT images were imported into a multimodality image registration software (Mirada XD, Mirada Medical Ltd, Oxford, UK), which includes a deformable registration module. A T2-weighted turbo spin echo transverse MR sequence was used for the CT and MR image registration. CT and MR images were first rigidly registered, and then elastic registration was performed using a mutual information algorithm. For the final registration, a qualitative evaluation was performed using the skin surface, skin marker, and bone structures. The operated breast soft tissue concordance was emphasized because CT and MRI were acquired with different breathing procedures, and spatial correspondence on the FOV was unachievable. The contouring of the whole breast and BST was performed by an experienced radiation oncologist (RO). The planning target volume (PTV) of the whole breast was an isotropic expansion of the clinical target volume (CTV) with a 7-mm margin in all directions, and the first 5 mm inside the body external contour were excluded from the CTV and PTV. The BST was delineated on CT images (BST$_{CT}$) and then on deformed MRI axial slices (BST$_{MR}$). Other imaging modalities were not used to create contours.

Treatment planning

CT and MR images and corresponding Dicom RT structures were exported to the Philips Pinnacle3 treatment planning system. All patients

were treated with 6-MV photon beams using a Siemens Artiste linear accelerator (Siemens Medical Solution, Erlangen, Germany). A dose of 45 Gy was prescribed to the PTV of the whole breast with a hypo-fractionated schedule of 16 fractions of 2.25 Gy each, and 50 Gy to the BST was concomitantly delivered in 16 fractions of 2.5 Gy per fraction, which is the standard in our institute. The plans were developed to ensure dosimetric coverage of the whole breast with at least 95% of the prescribed dose (42.75 Gy) to 95% of the PTV and at least 95% of the prescribed dose (47.50 Gy) to 95% of the BST. For the ipsilateral lung, we assessed the V20 and mean dose (Dmean), and for patients requiring left breast irradiation, we assessed the Dmean and V30 and V5 to the heart, where Vx is defined as the volume in percentage receiving x Gy. The ipsilateral lung V20 was kept under 10%, and the heart V25 and V5 were kept under 4.0% and 0.5%, respectively. For whole breast irradiation, two coplanar tangential semi-opposed wedged beams (usually virtual 15° or 30°) and a multileaf collimator were used. Beam angles, wedged angles, and beam weighting were chosen to optimize the coverage of the PTV while minimizing exposure to the ipsilateral lung, heart, and contralateral breast. For patients treated on the right side, the gantry angles ranged from 45° to 55° for the medial fields and from 225° to 230° for the lateral fields, whereas for left breast irradiation, the gantry angles from 305° to 320° for the medial fields and from 135° to 152° for the lateral fields were used. The virtual wedge was used in both the lateral and medial fields to improve dose homogeneity. To create a concomitant boost plan, two more photon beams were introduced and shaped around the BST_{CT} using the multileaf collimator; an automatic surrounding margin of 0.3 cm was applied.

Statistical analysis

The BST_{CT} and BST_{MR} were compared in terms of volume and positioning using the conformity index (CI),[6] which is the ratio of the overlapping volume to the encompassing delineated volume. A CI of 1 indicates 100% concordance on the volume and location of the SB, a CI of 0.50 indicates that the observers agreed on 50% of the encompassing delineated volume, and a CI of 0 indicates no concordance. For each patient, a dose volume histogram (DVH) was generated for all the structures considered. BST_{CT} and BST_{MR} coverages were compared using the volume covered by 98% of the prescribed dose (V98%). V98% differences in BST_{CT} and BST_{MR} were analyzed by the same RO.

Results

In patients who did not undergo chemotherapy, the interval between surgery and image acquisition ranged from 30 to 60 days, with a median of 37 days, whereas in patients who underwent adjuvant chemotherapy, the interval ranged from 45 to 178 days. The intervals between breast surgery and treatment planning imaging are reported in Table 1.

Good-quality MR images with minimal distortion were obtained in the supine position. Images were transferred to the Mirada RTx software with no difficulty. Axial T2 images were preferred for image registration. Using the MRI-CT deformable algorithm, we were able to fuse CT and MR images with very good results. Table 2 shows the CT and MRI boost volumes of each patient and their volume percentage difference. The volumes ranged between 15.5 cm³ and 226.6 cm³ for the CT images. The average volume reduction on MR images was 99%, with a range of 10%–450%. BST_{MR} was larger than BST_{CT} in only two patients [Table 2]. The

Table 1

Interval between surgery and imaging for treatment plan preparation.

Parameters	Interval length (days)		
	30–45	45–60	60–178
All patient	10	6	2
Patients receiving concomitant chemotherapy	0	2	2

BSTs differed not only in volume but also in localization inside the breast, with the CI ranging from 0.24 to 0.67. The coverage of BST_{CT} and BST_{MR} for a representative patient on the three planned orientations of MR images and the corresponding DVHs are portrayed in Figure 1; the dotted line indicates the difference in the V98% in the DVH. The impact of CI differences on the dosimetric coverage of the BST, in terms of V98%, is reported in Figure 2. The average V98% difference was only 10%, but the range was 2.8%–39.3%. Figure 3 shows the differences in the V98% as a function of the CI.

The highlighted point in Figure 3 corresponds to the breast seroma case, in which CT overestimated the boundaries of the SB, which was properly identified by MRI.[12] The BST_{CT} and BST_{MR} contours for the seroma case and the corresponding dose distribution are shown in Figure 4.

Discussion

In this study, we compared the volumes and corresponding dosimetry of the BST delineated on MRI and CT images for the treatment plan preparation. We found reduced volumes for BST_{MR} compared to BST_{CT}, considerable variation between the radiation volumes to the SB between CT images and MRI, and boost doses with V98% differences up to 30%. The BST_{CT} varied in terms of size, shape, and position within the breast. This may be due to the grade and location of the lesion and, consequently, the volume of the lumpectomy. The experience of the RO strongly affects the boost contouring of CT images.[4] This is related to the lack of intrinsic soft tissue contrast of CT and leads to a strong operator dependence on a procedure that should instead be repeatable and reproducible. The information obtained from MR images is more detailed, and a more precise definition of the SB may be obtained[13] with a subsequent reduction in the variability on boost delineation. Therefore, MRI can be used to identify only the area with the highest probability of containing the microscopic residual disease, which is a cause of recurrence, for inclusion in the target volume.

Our findings showed that the volumes contoured on MR images were smaller than the corresponding volumes on CT images, which is in agreement with the results of other studies.[14–16] Only two patients in our studies had a BST_{MR} larger than the corresponding BST_{CT} (14.3% and 16.08% larger, respectively). In these cases, the lumpectomy cavity was contoured on MRI following traces of edema or tissue imbibition, which are better detected on MRI, and the resulting volumes were expanded toward the lower part of the breast because of gravity. It should also be noted that these two patients underwent CT and MRI only 30 and 35 days after surgery, respectively. In this study, the MRI and CT boosts were

Table 2

Boost volume identified on MR (BST_{MR}) and CT (BST_{CT}) images and the percentage difference between BST_{CT} and BST_{MR}.

Patient No.	BST_{MR} (cm³)	BST_{CT} (cm³)	% Diff
1	12.2	15.5	26.7
2	24.7	28.8	16.7
3	16.1	33.3	106.2
4	30.5	33.7	10.5
5	9.8	34.4	251.8
6	16.9	35.2	108.5
7	52.9	36.1	−31.8
8	29.3	47.6	62.4
9	44.2	79.1	79.1
10	56.1	85.2	51.8
11	115.0	96.4	−16.1
12	48.9	108.7	122.7
13	118.2	156.3	32.3
14	124.3	165.5	33.2
15	142.8	166.0	16.2
16	32.7	179.8	449.5
17	120.5	199.4	65.4
18	69.2	226.6	227.7

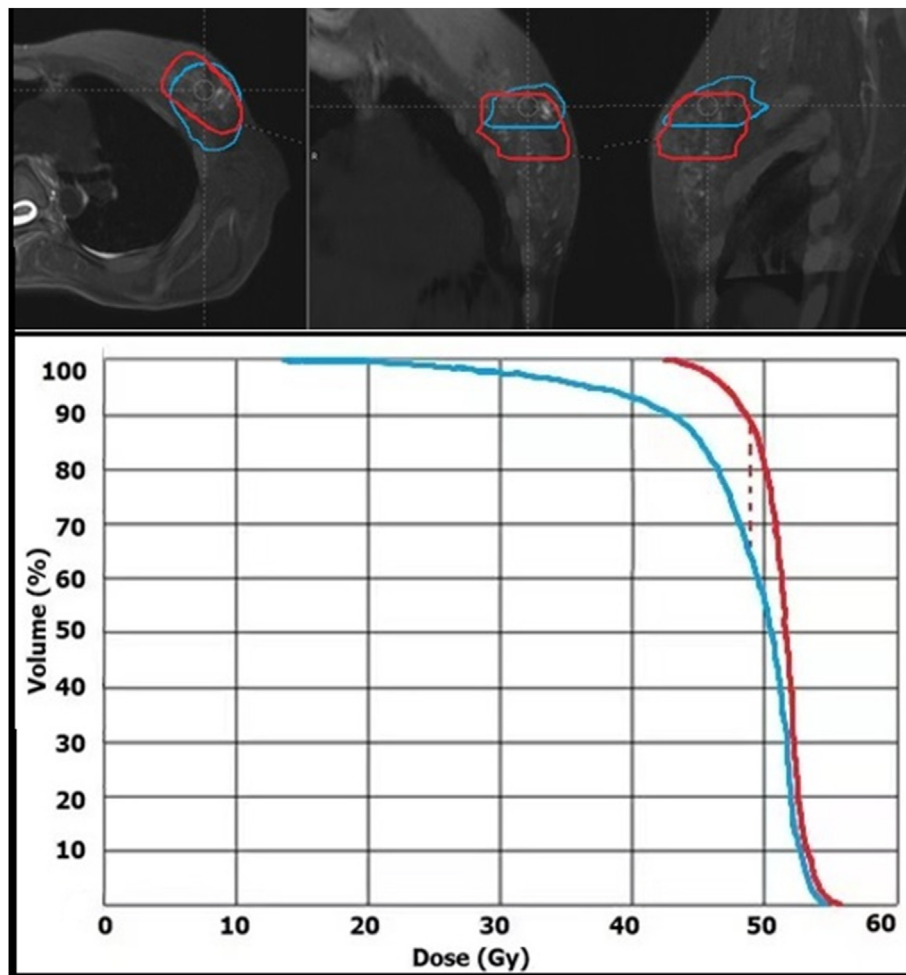MR: Magnetic resonance; CT: Computed tomography.

Figure 1. BST$_{CT}$ and BST$_{MR}$ contours in red and blue, respectively, for a representative patient on the three planned orientations of MR images and the corresponding DVHs. The red dotted line highlights the difference in the volumes covered by 98% of the prescribed dose (ΔV98%). BST: Boost volume; CT: Computed tomography; MR: Magnetic resonance; DVH: dose-volume histogram.
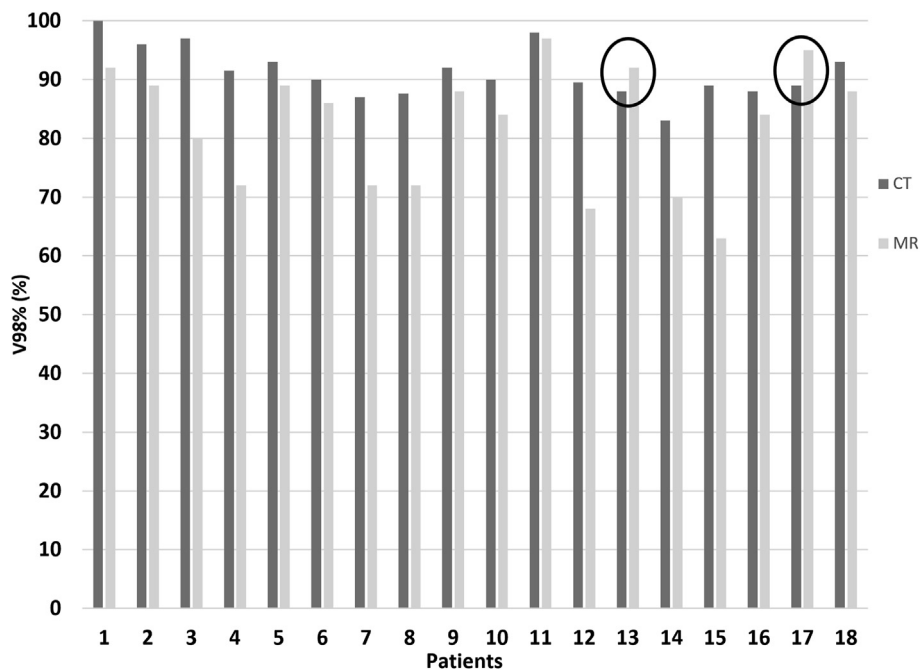

Figure 2. The V98% of the BST$_{CT}$ and BST$_{MR}$. The black circles indicate the only two patients for whom the BST$_{MR}$ was larger than the BST$_{CT}$. V98%: 98% of the prescription dose; BST: Boost volume; CT: Computed tomography; MR: Magnetic resonance.
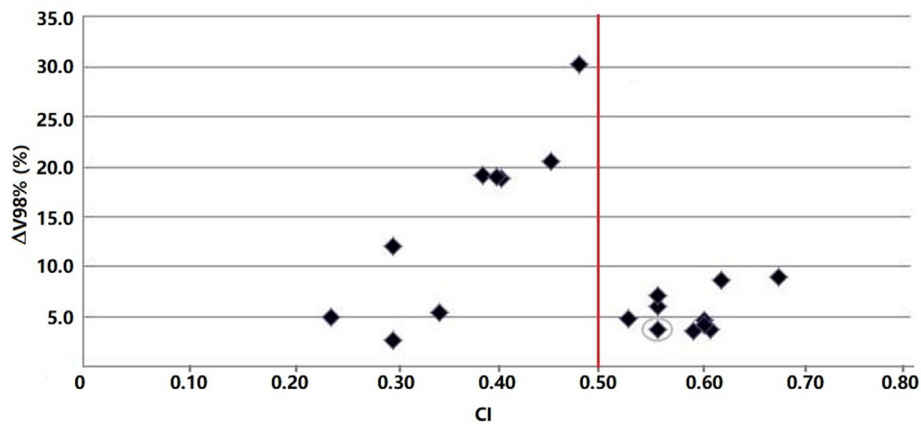
Figure 3. Absolute difference between the BST$_{CT}$ and BST$_{MR}$ V98% as a function of the conformity index (CI). The point corresponding to the seroma case has been circled. A red line indicating a CI of 0.50 has been added, at which point the observers agreed on 50% of the encompassing delineated volume. BST: Boost volume; CT: Computed tomography; MR: Magnetic resonance.

always embedded in the same quadrant of the breast, but the volumes and the locations varied because of the different intrinsic information coming from the different imaging modalities. This is reflected in the CI values, which take into account the inclusion and overlap volumes between MRI and CT boosts. The range of CI values was very wide (0.24–0.67), highlighting how the contouring of the boost on the two modalities differs not only in the volume but also in the location.

The impact of this variability on treatment is demonstrated by the difference in the V98% of the BST$_{CT}$ and BST$_{MR}$ for each patient. These differences are not strictly related to the CI because when the BST$_{MR}$ is smaller and completely enveloped by the BST$_{CT}$, the difference in V98% becomes negative, i.e., the BST$_{MR}$ is better covered than the BST$_{CT}$, as illustrated by the circled bar in Figure 2. The CI contains both the information about the translational difference of the boost centers and the difference in volume size but cannot differentiate between them, whereas the V98% reflects only the difference in coverage. This situation was common in our study. The CI and V98% difference data seemed to be split into two areas: CI > 0.50 and CI < 0.50, as shown by the red line in Figure 3. If the CI was <0.50, the difference in V98% was very large (ranging from 2.6% to 30.2%), indicating either that the CT and MRI volumes were comparable in size but differently located in the breast, which leads to a very low CI and a very high V98% difference, or that the two volumes were different (very low CI) but enveloped, leading to the same dosimetric coverage (very low V98% difference). If the CI was >0.50, the volumes were similar and overlapped well. Despite the good agreement between the MRI and CT boosts, there were differences in the V98% of 5–10%, which are small but still significant.

MRI provides greater detail than CT, showing heterogeneous cavities, concentric rings of granulation tissue, and the presence of edema and tissue imbibition; additionally, DWI is a powerful tool to characterize breast lesions because of its high specificity for differentiating benign and malignant lesions. However, its use in a clinical workflow of breast irradiation should be investigated, and multicenter randomized controlled trials are still necessary to assess its clinical value.[14] The
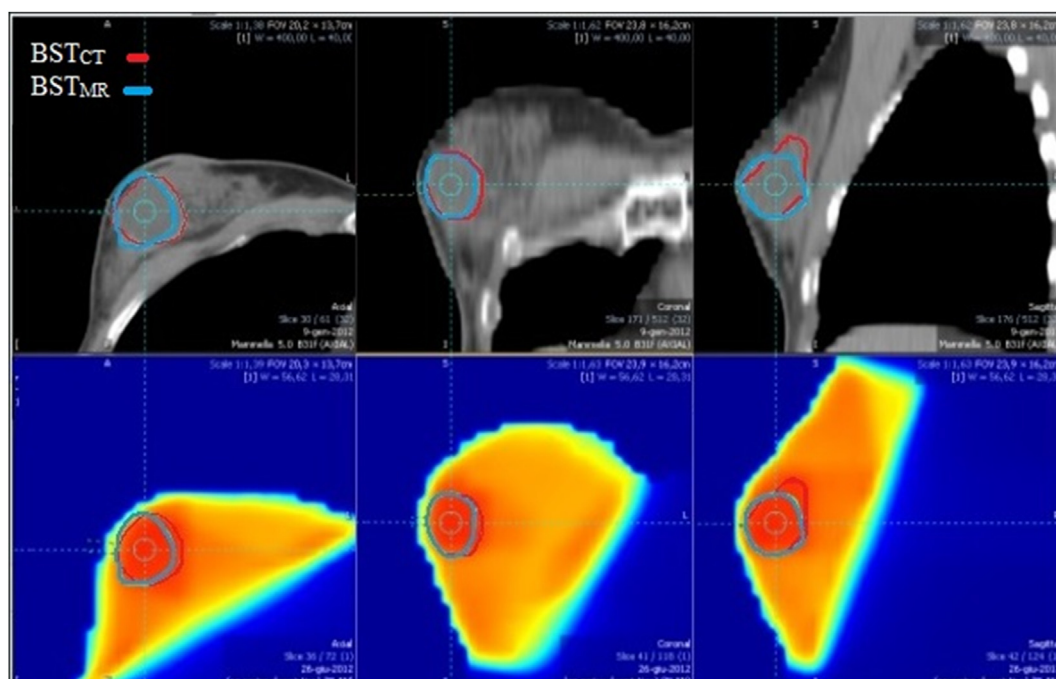

Figure 4. BST$_{CT}$ (in red) and BST$_{MR}$ (in blue) for the seroma case and the corresponding dose distribution. BST: Boos volume; CT: Computed tomography; MR: Magnetic resonance.

quasi-standardized procedure proposed in this work offers CT images as the geometric gold standard but adds additional anatomical information through elastic fusion with MR images. Although this procedure may seem too time-consuming and costly for the administration of 5 Gy of simultaneous boost irradiation, it may be meaningful if partial breast treatment is performed[17]; the visibility of the seroma on MRI facilitates its delineation as shown in the results; the use of MR-guided radiotherapy may be useful for monitoring volume changes over the treatment course, improving treatment accuracy.[18] Further investigations on how to identify the SB using MRI are still in progress.[19,20] MR-guided radiotherapy with MR-Linac can also be used; however, breast treatment may benefit from respiration-guided irradiation, which if not controlled could lead to dosimetric differences in the irradiation of the whole breast PTV. Therefore, although the MR-Linac technology may seem attractive, the entire treatment needs to be evaluated, and further investigations are necessary.

The study involved a limited number of patients coming from a single institution and it can be considered a small study; moreover, even if the contouring was performed by the same RO following international guidelines it was not validated by multi-institutional quality assurance program. Despite this, the study highlights the possibility of improving boost dosimetry through the use of MRI and CT images for treatment plan preparation.

In conclusion, the introduction in the clinical workflow of merged MR–CT imaging for breast RT treatment planning may provide important imaging insights for radiation oncologists for a precise lumpectomy cavity delineation to ensure a correct dose to the boost volume.

Funding

Author contribution

Study concept and design of the research: MB and LC. Acquisition of data and image dataset processing: CB, MB, and MD. Analysis and interpretation of data: LCO, LC, and MB. Manuscript preparation: MB, LCO, and CB. Manuscript writing: MB. Manuscript critical revision: LCO and MD. All authors read and approved the final manuscript.

Ethics statement

The authors declare that the study received the approval of the Ethics Committee of the Hospital Centro Oncologico Fiorentino, located in Via Attilio Ragionieri 1, Sesto Fiorentino Florence (Italy), where the data evaluation was performed. All patients provided consent for the elaboration of the study data and future scientific publication.

Data availability statement

The datasets generated and analyzed during the present study are not publicly available due to participant privacy but are available from the corresponding author on reasonable request.

Conflict of interest

None.

Acknowledgment

References

1. Laan HD, Dolsma WV, Maduro JH, et al. Three-dimensional conformal simultaneously integrated boost technique for breast-conserving radiotherapy. *Int J Radiat Oncol Biol Phys*. 2007;68:1018–1023. https://doi.org/10.1016/j.ijrobp.2007.01.037.
2. Landis DM, Luo W, Song J, et al. Variability among breast radiation oncologists in delineation of the postsurgical lumpectomy cavity. *Int J Radiat Oncol Biol Phys*. 2007;67:1299–1308. https://doi.org/10.1016/j.ijrobp.2005.07.020.
3. Logue JP, Sharrock CL, Cowan RA, et al. Clinical variability of target volume description in conformal radiotherapy planning. *Int J Radiat Oncol Biol Phys*. 1998;41:929–931. https://doi.org/10.1016/S0360-3016(98)00148-5.
4. Petersen RP, Truong PT, Kader HA, et al. Target volume delineation for partial breast radiotherapy planning: clinical characteristics associated with low interobserver concordance. *Int J Radiat Oncol Biol Phys*. 2007;69:41–48. https://doi.org/10.1016/j.ijrobp.2007.01.070.
5. Li X, Tai A, Arthur D, et al. Variability of target and normal structure delineation for breast cancer radiotherapy: an RTOG Multi-Institutional and Multiobserver Study. *Int J Radiat Oncol Biol Phys*. 2009;73:944–951. https://doi.org/10.1016/j.ijrobp.2008.10.034.
6. Struikmans H, Warlam Rodenhuis C, Stam T, et al. Interobserver variability of clinical target volume delineation of glandular breast tissue and of boost volume in tangential breast irradiation. *Radiother Oncol*. 2005;76:293–299. https://doi.org/10.1016/j.radonc.2005.03.029.
7. Goldberg H, Prosnitz RG, Olson JA, et al. Definition of postlumpectomy tumor bed for radiotherapy boost field planning: CT versus surgical clips. *Int J Radiat Oncol Biol Phys*. 2005;63:209–213. https://doi.org/10.1016/j.ijrobp.2005.01.044.
8. Whipp EC, Halliwell M. Magnetic resonance imaging appearances in the postoperative breast: the clinical target volume–tumor and its relationship to the chest wall. *Int J Radiat Oncol Biol Phys*. 2008;72:49–57. https://doi.org/10.1016/j.ijrobp.2007.12.021.
9. Ahn KH, Hargreaves BA, Alley MT, et al. MRI guidance for accelerated partial breast irradiation in prone position: imaging protocol design and evaluation. *Int J Radiat Oncol Biol Phys*. 2009;75:285–293. https://doi.org/10.1016/j.ijrobp.2009.03.063.
10. Kirby AM, Yarnold JR, Evans PM, et al. Tumor bed delineation for partial breast and breast boost radiotherapy planned in the prone position: what does MRI add to X-ray CT localization of titanium clips placed in the excision cavity wall? *Int J Radiat Oncol Biol Phys*. 2009;74:1276–1282. https://doi.org/10.1016/j.ijrobp.2009.02.028.
11. Jolicoeur M, Racine ML, Trop I, et al. Localization of the surgical bed using supine magnetic resonance and computed tomography scan fusion for planification of breast interstitial brachytherapy. *Radiother Oncol*. 2011;99:480–484. https://doi.org/10.1016/j.radonc.2011.08.024.
12. Wong EK, Truong PT, Kader HA, et al. Consistency in seroma contouring for partial breast radiotherapy: impact of guidelines. *Int J Radiat Oncol Biol Phys*. 2006;66:372–376. https://doi.org/10.1016/j.ijrobp.2006.05.066.
13. Vasmel JE, Koerkamp M, Kirby AM, et al. Consensus on contouring primary breast tumors on MRI in the setting of neoadjuvant partial breast irradiation in trials. *Practical Radiation Oncology*. 2020;10:e466–e474. https://doi.org/10.1016/j.prro.2020.03.011.
14. Chen X, Li WL, Zhang YL, et al. Meta-analysis of quantitative diffusion-weighted MR imaging in the differential diagnosis of breast lesions. *BMC Cancer*. 2010;10:693. https://doi.org/10.1186/1471-2407-10-693.
15. Huang W, AaC MD, Chen X, et al. A comparison of lumpectomy cavity delineations between use of magnetic resonance imaging and computed tomography acquired with patient in prone position for radiation therapy planning of breast cancer. *Int J Radiat Oncol Biol Phys*. 2016;94:832–840. https://doi.org/10.1016/j.ijrobp.2015.12.014.
16. Pogson EM, Delaney GP, Ahern V, et al. Comparison of magnetic resonance imaging and computed tomography for breast target volume delineation in prone and supine positions. *Int J Radiat Oncol Biol Phys*. 2016;96:905–912. https://doi.org/10.1016/j.ijrobp.2016.08.002.
17. Jacobson G, Zamba G, Betts V, et al. Image-Based treatment planning of the post-lumpectomy breast utilizing CT and 3TMRI. *International Journal of Breast Cancer*. 2011;2011:246265. https://doi.org/10.4061/2011/246265.
18. Jeon SH, Shin KH, Park SY, et al. Seroma change during magnetic resonance imaging-guided partial breast irradiation and its clinical implications. *Radiat Oncol*. 2017;12:1–7. https://doi.org/10.1186/s13014-017-0843-7.
19. Lowrey N, Koch CA, Purdie T, et al. MRI for breast tumor bed delineation: CT comparison and sequence variation. *Advances in Radiation Oncology*. 2021;6:100727. https://doi.org/10.1016/j.adro.2021.100727.
20. Muvvala M, Rapole PS, Karunanithi G, et al. Finding an alternative for the surgical clips-based delineation of tumor bed boost volume for radiotherapy after breast conserving surgery: a prospective comparative study. *Asian Pacific Journal of Cancer Care*. 2021;5:303–306. https://doi.org/10.31557/APJCC.2020.5.4.303-306.